JOURNAL OF APPLIED BIOANALYSIS, June 2017, p. 110-119.
http://dx.doi.org/10.17145/jab.17.014 (ISSN 2405-710X)
Vol. 3, No. 4

OPEN ACCESS

RESEARCH ARTICLE

Application of promising carbonaceous materials in electrochemical DNA sensing

Sophia Karastogianni[1], Eleni A. Deliyanni[2,*], Stella Girousi[1,*]

[1]*Analytical chemistry Laboratory, Chemistry Department, Aristotle University of Thessaloniki, Thessaloniki, Greece.*
[2]*Laboratory of Chemical and Environmental Technology, Aristotle University of Thessaloniki, Greece.*

(Received: 8 April 2017, Revised 23 May 2017, Accepted 28 May 2017).

The data reported in literature demonstrate that carbon paste electrodes (CPEs) are very suitable for a variety of applications and many works have thus been devoted in the development of new sensitive and selective electrode surfaces based on carbon paste as the electrode material of choice. The application of novel and promising carbonaceous materials, as electrode surfaces, is an issue of great concern. In this work the experimental results of the characterization and comparison of electrode surfaces based on alternatively prepared carbonaceous materials (activated carbon (B), HNO_3 oxidized activated carbon (B5), Ag impregnated activated carbon (B-Ag) and graphite oxide (GO), are being demonstrated. Scaning Electron Microscopy SEM), surface acidity, FTIR spectroscopy, XRD diffractometry and electrochemical techniques (cyclic voltammetry, differential pulse voltammetry) were applied in the characterization of novel carbonaceous materials aimed at electrochemical DNA sensing.

Keywords: characterisation, carbonaceous materials, scanning electron microscopy, surface acidity, FTIR spectroscopy, X-ray powder diffraction, cyclic voltammetry, differential pulse voltammetry, DNA sensing.

Introduction

Engineered nanostructures nowadays are still in the center of the interest because of their unique novel properties, based in their nano-dimension, produce functional and efficient new technological devices [1]. Nevertheless they are connected with exposure risks to envious organisms from simple cells to humans. Physicochemical properties as size, surface charge, surface area, solubility, ligands play important roles at the bio-interactions of nanostructures [2] and have extremely importance about biocompatibility and toxic effects. Especially size by the inverse relationship with surface area can increase the reactivity of a material with the target that comes in contact. The so called "size effects" as surface reactivity play key role for the bio-distribution, cellular uptake, internalization and activation of intracellular toxicity factors and signals and also other bio-interactions influencing cytotoxicity [3-5] biocompatibility and bio-functionality.

Electrochemical technique has been considered as the best candidate for the on-site detection of molecules such DNA due to the high sensitivity, simplicity, reproducibility, low cost, relatively short analysis time and direct analysis, without any extraction, clean-up or preconcentration steps, and easy to miniaturization [6]. The ease and speed of preparation and of obtaining a new reproducible surface, the low residual current, porous surface and low cost of carbon paste are advantages of carbon paste electrode (CPE) over all other solid electrodes [7]. Furthermore, carbon is compatible with biological tissues more than other materials and as a result has broad application in electrochemical DNA sensors [7-12]. Thus, carbon paste, in both unmodified and modified forms, is

***Correspondence:**
Analytical chemistry Laboratory, Chemistry Department, Aristotle University of Thessaloniki, Thessaloniki 54124, Greece. Phone: +30 2310997722; fax: +30 231997719; E-mail: girousi@chem.auth.gr

a material that has been widely utilized for electrochemical detection of biomolecules.

Due to their principally advantageous properties, carbon materials are being used in a variety of carbon electrodes, particularly for electroanalysis and electrosynthesis [8]. The advantageous properties of these carbon-based electrodes include wide potential windows, fairly inert electrochemistry, and good electrocatalytic activity for many redox reactions [9]. Meanwhile, graphitic carbon material with micro or mesoporous textures and high surface area have attracted attention because of their potential use in field emission, catalyst support, super capacitors, adsorption and solar energy. Based on their excellent electronic properties, antifouling properties, and ability to promote electron transfer reactions graphitic carbon materials also find interesting applications in biosensing devices. In addition, due to their bioselectivity for redox enzymes, these materials have been proven to be very useful for the quantification of organic substances such as glucose [13], proteins [14], hydroquinone [15] as well as antioxidant activity [16,17].

Activated carbonis, a black, solid, biocompatible carbonaceous material is commonly obtained from various organic precursors such as peat, wood, bituminous coal, coconut shells, petroleum pitch, polymers etc. [14,15]. Variations in the conditions of the manufacturing process of activated carbons allow the generation of numerous types of them which differ in their basic features like surface area, porosity, surface chemistry etc. Thus, with activation, its properties can be easily changed to have large internal as well as specific surface area and porosity, high density of carbon in graphite-like layers, resulting in high mechanical strength [16]. Activated carbon-based systems can remove a large variety of pollutants from the solution phase with great efficiency [17]. To further develop highly efficient materials for various applications like adsorption or electrochemical sensors, modification of activated carbon [18] has received considerable attention. Among them, metal ion-loaded carbons show great application potential [18]. The metals such as Ag incorporated to the surface act not only as active sites for selective adsorption of sulfur-containing aromatic compounds but also as structural stabilizers of the carbon materials and as catalyst initiators in reactive adsorption. Hence, activated carbon surfaces with Ag could be used to improve the properties of existing electrodes. Moreover, they can be used in the development of electrochemical DNA biosensors [19, 20-28]. To the best of our knowledge, this is the first time that wood-based activated carbon modified CPE or Ag impregnated wood-based activated carbon modified CPE have been used in DNA electrochemical sensing.

Graphite oxide (GO) is a graphite derivative with covalently attached oxygen-containing groups to its layers. These groups are generated in the course of the GO synthesis by strong oxidation [29]. In this sense, GO exhibits lamellar structure with randomly distributed unoxidized aromatic regions (sp^2-carbon atoms), six-membered aliphatic regions (sp^3-carbon atoms) as a result of oxidation, and a high concentration of exposed oxygen-containing functional groups, like hydroxyl, epoxy, and carboxyl, embedded in its carbon layers [29]. Although not fully verified, it has been proposed that the epoxy and C-OH functional groups lie above and below each carbon layer, while the-COOH groups are located near the layers' edges [29]. Owing to the presence of such hydrophilic polar groups in the solid, GO is quite reminiscent of montmorillonites, which share common swelling and intercalation properties. As a result, GO is an excellent host matrix for the interlayer accommodation of long chain aliphatic hydrocarbon [30] and hydrophilic molecules and polymers [31] and is also promising for particle engineering processes, especially for the fabrication of thin films with smart properties [32]. Based on these excellent characteristics, GO is also promising in the modification of electrode surfaces, and therefore it can be used in the detection of DNA. Up to now, only few reports [33] have been used graphite oxide modified CPE in DNA electrochemical sensing.

Given the wide use of activated carbons and graphite oxide, in this work the experimental results of the characterization of electrode surfaces based on alternatively prepared carbonaceous materials (micro-mesoporous wood-based activated carbon (B), HNO_3 oxidized (B5) and Ag impregnated derivatives of B carbon BAX-Ag (B-Ag) as well as graphite oxide (GO), are being demonstrated. SEM, FTIR, XRD, surface acidity and electrochemical techniques (cyclic voltammetry, differential pulse voltammetry) were applied in the characterization of novel carbonaceous materials' electrodes aimed at electrochemical DNA sensing.

Materials and methods

All the chemicals used were reagents of analytical grade unless stated otherwise. Ethylene diamine tetra-acetic EDTA, ACS, reagent 99.4-100.06 % was obtained from Sigma – Aldrich and tris 99.8 % was ACS reagent. Double stranded (ds) calf thymus DNA (D-1501, highly polymerized) was purchased from Sigma, Chemical, CO (St Louis, MO, USA). The dsDNA stock solution (1000 mg/L) was prepared 10 mmol/L Tris-HCL and 1 mmol/L EDTA pH 8.0. All aqueous solutions were prepared with

doubly-distilled water. Graphite powder was purchased from Fluka (50870, p.a. purity 99.9 % and particle size < 0.1 mm). The activated carbon used was a wood-based activated carbon BAX-1500, manufactured by Mead Westvaco, USA.

GO was prepared in the laboratory according to the modified Hummers method [34]. Commercial graphite powder (10 g) was stirred in concentrated solution of sulfuric acid (230 mL, 0 ºC) and then 30 g of potassium permanganate was slowly added to the suspension. The addition rate was controlled in order the suspension's temperature was less than 20 ºC. Distilled water (230 mL) was slowly added to the reaction vessel, keeping the temperature less than 98 ºC and after further dilution with 1.4 L of distilled water was realized 100 mL of 30 wt % hydrogen peroxide were added. GO particles, settled at the bottom were separated from the excess liquid by decantation and were transferred to a dialysis tube. The final gel like material, separated by centrifugation was freeze-dried and the dark brown powder of GO was obtained.

For the preparation of the oxidized carbon sample, B carbon was oxidized with 70 % (v/v) HNO_3 for 5 h (carbon denoted hereafter as B5). The excess of acid and the soluble products of surface oxidation were removed by washing with water at 100 ºC using a Soxhlet apparatus, until constant pH. The preparation of Ag impregnated B carbon sample (carbon denoted as B-Ag) was made according to the Tollens method [35].Concentrated NH_4OH was slowly added to 100 mL of 0.23 mol/L $AgNO_3$ solution under stirring. After the formed brown precipitate (Ag_2O) was dissolved, 50 mL of 1.84 mol/L NaOH were added followed by slowly addition of concentrated NH_4OH until a colorless silver diammine complex ($[Ag(NH_3)_2]^+$) was formed. A volume of the resulting solution (50 mL) was added to 5 g of B carbon. The mixture, after stirring for 24 h, was filtered and oven dried at 120 ºC. The Ag content of this carbon is 10 wt %.

The purity of DNA was check by monitoring the ratio of the absorbance at 260-280 nm. The solution gave a ratio of A266/A280 >1.8 indicating that DNA was sufficiently free from proteins. All solutions were stored in refrigerator at 10 ºC.Voltammetry experiments for electrode characterization and the DNA study were carried out using μAutolab potentiostat/galvaniostat controlled by GPES 4.9 software 9 (EcoChemie, TheNetherlands). The electrochemical experiments were carried out in a three electrode glass cell system with platinum wire (Metrohm, Switzerland) as counter electrode and Ag/AgCl as a reference (MF-2052 BASI). On one hand the working electrode was the unmodified carbon paste electrode (CPE), prepared by hand mixing graphite powder to mineral oil by 75/25 ratio. On the other hand the working electrode was prepared by hand mixing graphite powder to the alternative carbons (wood-based activated carbon, wood-based oxidized activated carbon, and wood-based Ag impregnated activated carbon as well as graphite oxide) and mineral oil by 80/20 ratio. The resulted paste was placed into a Teflon sleeve. All the electrochemical experiments were performed at ambient temperature in an electrochemical cell. The electrochemical cell was cleaned with diluted nitric acid and rinsed with sterilized double-distilled water.

X-ray powder diffraction (XRD) patterns were recorded with a XRD-diffractometer (model Richard Seifert 3003 TT, Ahrensburg, Germany) with a Cu Kα radiation (λ= 0.15405 nm). The samples were scanned from 5º to 60º. Scanning electron microscopy (SEM) images were recorded with electron microscope (model Zeiss Supra 55 VP, Jena, Germany) at an accelerating voltage 15.00 kV and in situ scanning on a sample powder. Potentiometric titration was performed with a Mettler Toledo T50 automatic titrator under N_2 atmosphere over a wide range of pH. The surface charge of the samples, Q (mmol/g), was calculated by the following **equation 1** [36]:

$$Q = \frac{C_A + C_B + C_{H^+} + C_{OH^-}}{W}$$

Where: C_A and C_B represent the acid (CA) and base (CB) concentrations (mol/L), C_{H+} and C_{OH-} the equilibrium concentrations of these ions (mol/L), and W the carbonaceous material concentration (g/L).

The amount of surface functional groups was measured according to the Boehm titration method [37]. The free acidic groups were calculated based on the assumption that: (i) $NaHCO_3$ neutralized only carboxyl groups; (ii) Na_2CO_3 neutralized carboxyl and lactonic groups, and (iii)NaOH neutralized carboxyl, lactonic and phenolic groups. The excess of base or acid was then determined by back titration using NaOH (0.10 mol/L) and HCl (0.10 mol/L) solutions [37].

The FTIR spectra of the carbonaceous samples were taken with a Nicolet 560 (Thermo Fisher Scientific Inc., MA, USA) FTIR spectrometer. The spectra were recorded in transmission mode using KBr pellets, from 4000 to 400/cm at a resolution of 4/cm.

For the measurement of the surface pH of carbon samples, 0.4 g of carbon sample were dispersed to 20 mL of deionized water; the suspension was stirred overnight to reach equilibrium and then the pH was measured. This method provided information about the acidity or basic-

ity of the carbon's surface. The voltammetric characterization of novel carbonaceous electrodes were carried out by cyclic voltammetry (CV) measurements, using the well studied redox reaction of $K_3[Fe(CN)_6]$ 0.05 mol/L and KCl 0.1 mol/L as supporting electrolyte [38]. The scanning potential was ranged from – 0.6 V to +0.6 V vs. Ag/AgCl. It has been characterized 20%, 40%, 80% w/w ratio between conventional graphite powder and the novel carbonaceous materials.

A three step procedure was used to study the dsDNA performance on modified CPE with novel carbonaceous materials. Firstly, the modified CPE with the novel carbonaceous materials was pretreated before every electrochemical measurement by applying potential +1.7 V vs. Ag/AgCl for 60 s in 0.2 mol/L acetate buffer solution containing 0.02 mol/L NaCl, a procedure that produce more hydrophilic surface and removes organic layers [39].Then, dsDNA was immobilized on the electrodes' surface by applying +0.5 V for 300 s and immersing the pretreated electrodes in 0.2 mol/L acetate buffer solution pH 4.5 containing 0.02 mol/L NaCl and the appropriate amount of dsDNA. Finally, signal transduction step was followed, using adsorptive transfer stripping voltammetry in 0.2 mol/Lacetate buffer solution pH 4.5 containing 0.02 mol/L NaCl, scanning the potential from +0.0 to +1.4 V with a step potential of 0.005 V, a E_{pulse} = 0.025 V and scan rate = 0.050 V/s. The characteristic oxidation peak potential of guanine residues was found at +1.1 V and used as the analytical signal for subsequent measurements.

Results and discussion

Although the porous structure and surface chemistry of the under examination carbonaceous materials has been already described [25,40,41], previously published results are briefly referred here along with new experimental results.

The XRD patterns of GO, and B-Ag, are shown in **Figure 1**. As seen in Figure B carbon presented to be amorphous as well as B5 carbon (not presented). The B-Ag carbon sample presented well defined peaks at 2θ = 38.28°, 44.61°, 64.50° and 77.62° assigned to the (111), (200), (220), and (311) lattice reflections of the face centered cubic (fcc) structure of silver [42,43]. The size of the silver nanoparticles, estimated from the Scherrer equation [35], found to be approximately 6–7 nm.

In the XRD pattern of GO the characteristic peak of GO was appeared at about 2θ = 11° indicating an interlayer distance of D1= 0.81 nm between the carbon layers, as determined by Bragg's law [44].The surface structure of B and GO are presented in their SEM images in **Figure 2**. The structure of GO exhibited the typical form of sheet-like structure while the activated carbon image presented cavities without any smooth surface area, typical image of the heterogeneous surface of carbons.

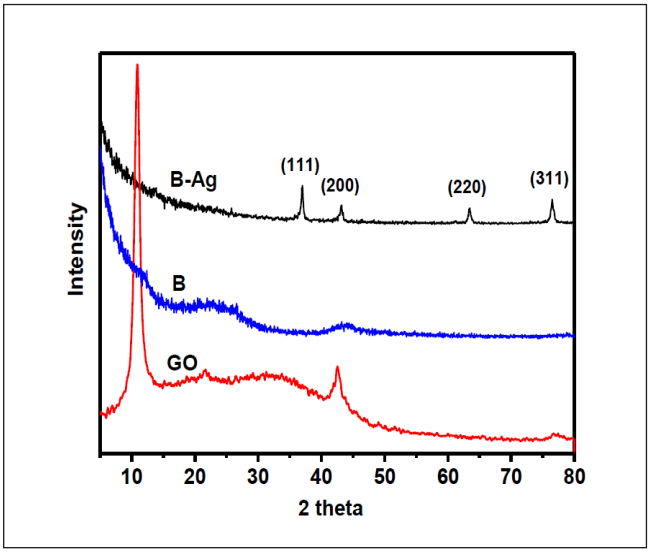

Figure 1. X-ray diffraction (XRD) patterns of: B, B-Ag and GO.

The parameters of the porous structure for all carbonaceous samples collected from previous published results [40, 41] are presented in **Table 1**. It was observed that the oxidation of B carbon as well as the impregnation with silver nanoparticles resulted in significant changes in the surface area and porosity of B5 and B-Ag carbons i.e. decrease of specific surface area (SBET) and pore volume. This decrease could be attributed to oxygen surface functional groups, for B5 and silver nanoparticles, for B-Ag, deposited in the carbon pore system.

Surface pH results of all carbon samples are presented in **Table 2**. It is seen that carbon oxidation resulted in decrease of the surface pH of the oxidized sample. This can be attributed to the deposition of oxygen functional groups on carbon surface which increased its acidic character. For the B-Ag carbon sample, Ag impregnation resulted in an increase of surface pH.

Table 1. Parameters of the pore structure calculated from nitrogen adsorption isotherms.

Samples	SBET m^2/g	V_{total} cm^3/g	V_{micro} cm^3/g	V_{meso} cm^3/g
B	2143	1.494	0.502	0.992
B5	1276	0.847	0.367	0.480
B-Ag	1680	1.000	0.390	0.610
GO	20.93	0.088	0.065	0.024

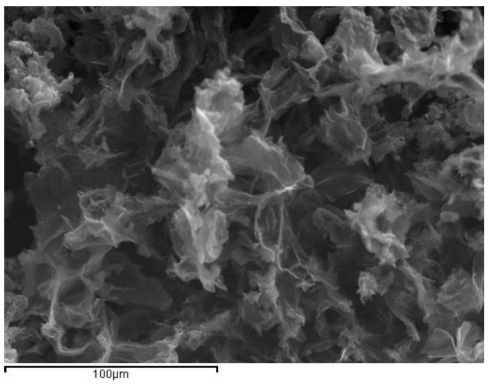

(a)

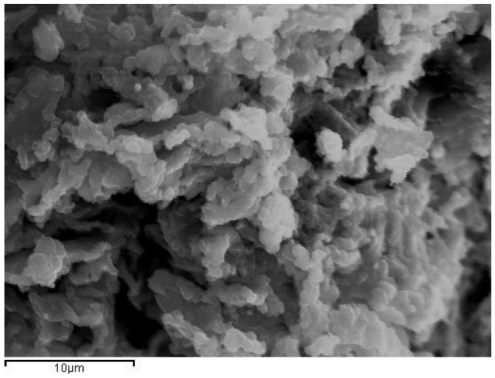

(b)

Figure 2. SEM images of (a) B activated carbon and (b) GO.

GO was the most acidic carbonaceous sample since pH for this sample presented the lowest value.

The acid character of these carbonaceous samples **are** also seen in the proton-binding curves, presented in **Figure 3**, which reveal that oxidation of B activated carbon caused an increase in surface acidity since the proton-binding curve for this sample shifted toward lower pH values comparing to the proton-binding curve for B carbon. The pH values variations of the raw and oxidized carbon are consistent with the proton uptake curves. The proton-binding curve for GO appeared at lower pH values than the proton-binding curve for B5 carbon. Again, the pH value of GO is consistent with the proton uptake curves. Our experimental data are in good agreement with already published results [40].

The amount of oxygen surface functional groups (lactonic, carboxyl and phenolic groups), as well as the amount of total acidic groups, were estimated by Boehm titration and the results are presented in **Table 2**. The results revealed the increase of acidic groups after oxidation, results consistent with the decrease of surface pH values and the proton binding curve for the B5 carbon. Oxidation resulted in pH decrease due to the increase of total oxygen functional groups, which was about 140 % for this sample. GO presented about double number of total acidic groups than B5; this sample presented the better performance indicating that surface acidity is an important parameter.

FTIR spectroscopy can also support the differences of the surface chemistry of the under examination carbonaceous materials. The surface chemistry of graphite oxide (GO), of the raw B carbon, the oxidized (B5) and the Ag impregnated carbon (B-Ag) were analyzed and the spectra are presented in **Figure 4.** For the raw B carbon the bands presented in the spectrum can be attributed to: C=C vibrations in the aromatic rings at 1590/cm, carboxyl C=O at 1700/cm, the carboxylic anhydrides at 1050/cm and carboxyl C–O and C–OH at 1350 and 1180/cm respectively [45]. Oxidation led to the formation of new surface functional groups. In the spectra of the B5 carbon, the bands attributed to carboxyl groups were strongly enhanced. New bands are also visible at 1560 and 1580/cm, attributed to stretching vibrations of C=O and C=C. Wide bands at 1050 and 1150/cm was assigned to phenolic O-H groups. After silver impregnation, the bands at 1350/cm representing carboxylic groups, increased. This can come as a result of oxidation

Table 2. Surface pH of the carbonaceous samples and Boehm titration results.

Samples	Surface pH	Carboxyl groups mmol/g	Lactonic groups mmol/g	Phenolic group mmol/g	Total acid groups mmol/g
B	5.2	0.208	0.105	0.478	0.790
B5	2.5	1.145	0.521	0.220	1.880
B-Ag	9.7	nd*	nd*	nd*	nd*
GO	2.1	2.431	0.904	0.717	4.052

*nd: not detected.

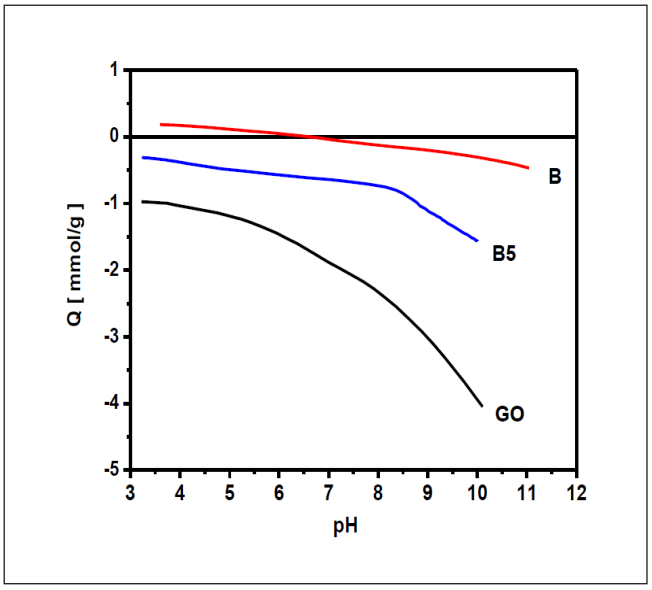

Figure 3. Potentiometric titration curves of the raw (B), oxidized activated carbon (B5) and graphite oxide (GO).

of active oxygen functional groups. Moreover, the changes are observed for the N–H bend of NH_3 that could be seen between 1650 and 1580/cm and the N–H wag, at 900–600/cm [46, 47]. The latter bands could also be assigned to Ag–O vibrations [48].

For GO spectrum, the bands at about 1050 and 1760/cm can be attributed to carboxyl groups, whereas the band at ~1600/cm to C=C stretching vibration of the sp^2 carbon skeletal network. The band at 1380/cm can be attributed to O-H groups (C-OH stretching), while the band at 1055/cm could be mainly attributed to epoxy groups. The peak at about 1220/cm might be due to S=O asymmetric stretching vibrations in sulfones or sulfates formed after graphite oxidation.

CV has been used to electrochemically study the new carbonaceous materials (B, B5, B-Ag and GO), which have been used as surface modifiers of CPE, using $K_3[Fe(CN)_6]$ as the redox probe, **Figure 5**. As it is seen in **Figure 5,** CPE (green line in **Figure 5**), has a pair of well-defined voltammetric peaks with cathodic peak potential (Epc) at around +0.095 V and anodic peak potential (Epa) at around +0.295 V. Meanwhile, B-CPE (black line in **Figure 5**), has also a pair of well-defined voltammetric peaks with cathodic peak potential (E_{pc}) at around +0.050 V and anodic peak potential (E_{pa}) at around +0.350 V. What is more, B5-CPE (red line in **Figure 5**), has also a pair of well-defined voltammetric peaks with cathodic peak potential (E_{pc}) at around +0.092 V and anodic peak potential (E_{pa}) at around +0.295 V. In addition, GO-CPE (blue line in **Figure 5**) has a pair of well-defined voltammetric peaks with cathodic peak potential (E_{pc}) at around +0.092 V and anodic peak potential (E_{pa}) at around +0.295 V. Furthermore, B-Ag-CPE (turquoise line in **Figure 5**) doesn't exhibit has a pair of well-defined voltammetric peaks, but two broad peaks with cathodic peak potential (E_{pc}) at around -0.001 V and anodic peak potential (E_{pa}) at around +0.400 V, which means that the redox system behavior is irreversible. The peak currents are increased and the peak-to-peak separation (ΔE_p) is nearly constant from 200 mV to 203 mV by use of B5-CPE and GO-CPE (red and blue lines, respectively), while is increased from 200 to 300 mV and to 401 mV by use of B-CPE and B-Ag-CPE, respectively (black and turquoise lines, respectively).

To calculate surface area of the electrodes the Randles-Sevcik equation was used (**equation 2**)

$$I_p = 2.69 \times 10^5 A D^{1/2} n^{3/2} v^{1/2} C$$

where n is the number of electrons transferred in the half reaction, A is the electrode surface area (cm^2), C is the bulk concentration of the analyte (mol/cm^3),υ is the scan rate (V/s), and D is the diffusion coefficient of the analyte in the solution (cm^2/s). From the Randles–Sevcik equation (**equation 2**) the surface area of the CPE and modified CPE with the novel carbonaceous materials can be calculated by substituting the values of D, n, υ and C. For the studied system ($K_3[Fe(CN)_6]$), n = 1, D = 7.6 ×

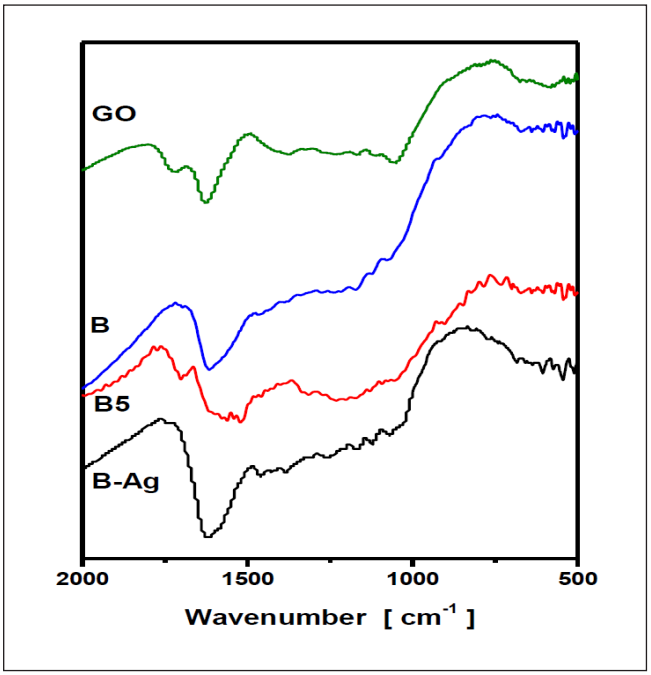

Figure 4. FTIR spectra for GO, raw (B) and oxidized carbon sample (B).

Table 3. Electrode surface area per weight ratio of the studied carbonaceous materials with conventional graphite powder.

Carbonaceous material	Ratio		
	20 %	40 %	80%
B	1.99×10^{-5}	2.65×10^{-5}	3.81×10^{-5}
B5	3.28×10^{-5}	2.60×10^{-5}	1.33×10^{-5}
B-Ag	2.36×10^{-5}	2.49×10^{-5}	2.57×10^{-5}
GO	2.70×10^{-5}	3.51×10^{-5}	3.74×10^{-5}
CPE		3.37×10^{-5}	

10^{-6} cm^2/s, thus the surface areas of the modified CPEs are calculated and shown in **Table 3** for different ratio of CPE and the respective carbonaceous material. As it can be seen from **Table 3** the surface area is decreased compared to conventional CPE when 20 % of all of the studied carbonaceous materials is used in the paste mixture. In addition, the surface area is also decreased compared with conventional CPE when 40 % of B-CPE, B5-CPE and B-Ag-CPE are used in the paste mixture, whilst the surface area is increased in the case of GO-CPE. On the other hand, the surface area is also decreased compared with conventional CPE when 80 % of B and B-Ag-CPE are used in the paste mixture, while the surface area is increased in the case of B5-CPE and GO-CPE. Thus, this ratio is used for subsequent experiments. All these results suggested strongly that carbonaceous materials modified carbon paste electrodes enhance the current responses of $K_3[Fe(CN)_6]$, with the exceptions of B5 where the current respond remains almost constant and of B-Ag-CPE where the current response is decreased. Moreover, the use of carbonaceous materials in the paste makes their electrode reactions more reversible in comparison

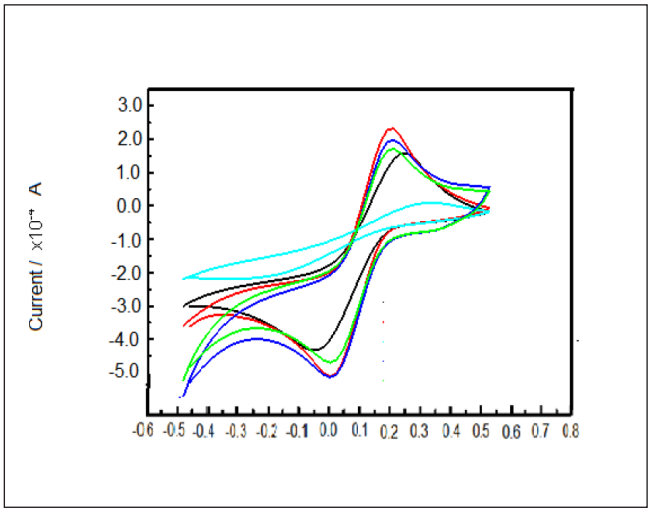

Figure 5. Cyclic Voltammetry characterization of GO at 0.05 V/s: B5 (black line), Bax (red line), CPE (green line), Bax_Ag (turquoise line) and GO (blue line) electrodes.

with those of CPE, with the exception of B-Ag-CPE. Differential pulse voltammetry (DPV) was used to study the analytical features of the modified CPE electrodes with the novel carbonaceous materials.

The diagnostic performance of the proposed DNA electrochemical biosensor was studied using the oxidation signal of guanine's residue of dsDNA in all of the cases of carbonaceous materials and the results are presented in **Table 4**. The results deduced from **Table 4**, concerning the linear range, the regression coefficient, the limit of detection as well as the limit of quantification, are indicative of the good analytical performance of the newly developed carbonaceous electrodes, which make them a promising tool allowing quantification of DNA. Furthermore, the relative standard deviation (s_r) measured at

Table 4. Comparison of the efficiency of various electrodes in the determination of vitamin B12.

Carbonacous electrode	Intercept of calibration plot	Slope of calibration plot	Linear range (mg/L)	Limit of detection (mg/L)[a]	Limit of quantifiction (mg/L)[b]	r	S_r[c] (%)
B-CPE	25.67 ± 0.945	2.686 ± 0.016	3.520 − 268.2	1.162	3.520	0.9998	3.8
B-Ag-CPE	72.44 ± 1.157	2.644 ± 0.020	4.347 − 209.6	1.143	4.374	0.9998	5.3
B5-CPE	41.95 ± 2.037	3.839 ± 0.035	5.305 − 100.0	1.751	5.305	0.9998	5.5
GO-CPE	65.28 ± 3.086	4.605 ± 0.054	6.701 − 156.8	2.211	6.701	0.9997	5.2
CPE	–[a]	–	–	–	–	–	–

[a]The limit of detection was calculated by means of $3.3s_b/a$, where s_b and a represent the standard deviation of the intercept and the slope of the calibration plot; [b]The limit of quantification was calculated by means $10s_b/a$, where s_b and a represent the standard deviation of the intercept and the slope of the calibration plot; [c]The relative standard deviation (s_r) was measured at 85.0 mg/L in all of the cases.; [d]There were deviations from linearity.

85.0 mg/L in all of the cases of carbonaceous materials was ranged from 3.8 and 5.5 % (see **Table 4**) indicating a remarkable reproducibility of the proposed biosensors. It must be noted that, B-CPE had the better analytical performance than the other electrodes (lower limits of detection and quantification, broader linear range and smaller standard deviation), followed by B-Ag-CPE, B5-CPE and GO-CPE, accordingly, **Table 4**.

Conclusions

To sum up, in the present work, combining the ability of activated carbon and graphite oxide to promote the adsorption and the electron-transfer reactions, a paste electrode based on these carbonaceous materials has been prepared and used for the study of dsDNA.The proposed carbonaceous materials had excellent ability to interact with dsDNA. They were found to be great electron transfer mediators, since the electrochemical results show that in most of the cases they pose reversible redox characteristics.In addition, the present results suggest that the new fabricated dsDNA modified electrode is a promising tool allowing direct quantification of DNA that can be included into future electroanalytical gene diagnosis platforms, or pharmaceutical testing, environmental and quality control, avoiding the high cost, low sensitivity, and procedural complication.

References

1. USEPA. Economic Analysis of the Proposed Change in Data Requirements Rule for Conventional Pesticides. (US Environmental Protection Agency, 2004).
2. Maynard A, Eileen D, Kuenpel D. Airborne nanostructure particle and occupational. J Nanopart Res 7, 587-614 (2005).
3. Lundqvist M, Stigler J, Elia G, Lynch I, Cedervall T, Dawson KA. Nanoparticle size and surface properties determine the protein corona with possible implications for biological impacts. Proc Natl Acad Sci USA 105, 14265–142704 (2008).
4. Wichmann HE, Spix C, Tuch T, Wölke G, Peters A, Heinrich J, Kreyling WG, Heyder J. Daily Mortality and Fine and Ultrafine Particles in Erfurt, Germany. Part I: Role Of Particle Number And Particle Mass. Research Report 98: Health Effects Institute: Boston, MA, USA, (2000).
5. Varna M, Ratajczak P, Ferreira I, Leboeuf C, Bousquet G, Janin A. In vivo distribution of inorganic nanoparticles in preclinical models. J Biomater Nanobiotechnol 3,18986 (2012).
6. Labuda J, Korgová H, Vaníčková M. Theory and application of chemically modified carbon paste electrode to copper speciation determination. Anal Chim Acta 305(1-3), 42-48 (1995).
7. Diculescu VC, Chiorcea-Paquim AM, Oliveira-Brett AM. Applications of a DNA-Electrochemical Biosensor. Trends Anal Chem 79, 23–36 (2016).
8. Fojta M, Daňhel A, Havran L, Vyskočil V. Recent Progress in Electrochemical Sensors and Assays for DNA Damage and Repair. Trends Anal Chem 79, 160–167 (2016).
9. Labuda J, Vyskocil V. DNA/Electrode Interface, Detection of Damage to DNA Using DNA-Modified Electrodes. In: Encyclopedia of Applied Electrochemistry (Eds: Kreysa G., Ota K., Savinell R.F.), Springer Science+Business Media, New York, pp. 346–350 (2014)
10. Vyskočil V, Hájková A. Novel Electrochemical DNA Biosensors as Tools for Investigation and Detection of DNA Damage. In: Bioanalytical Reviews (Ed: Matysik F.-M.), Vol. 6, Springer International Publishing, Cham, pp. 203–221 (2016).
11. Vyskočil V, Labuda J, Barek J. Voltammetric Detection of Damage to DNA Caused by Nitro Derivatives of Fluorene Using an Electrochemical DNA Biosensor. Anal Bioanal Chem 397, 233–241 (2010).
12. Hlavata L, Benikova K, Vyskocil V, Labuda J. Evaluation of Damage to DNA Induced by UV-C Radiation and Chemical Agents Using Electrochemical Biosensor Based on Low Molecular Weight DNA and Screen-Printed Carbon Electrode. Electrochim Acta 71, 134–139 (2012).
13. Lu J, Drazal LT, Worden RM, Lee I. Simple fabrication of a highly sensitive glucose biosensor using enzymes immobilized in exfoliated graphite nanoplatelets nafion membrane. Chem Mater 19(25), 6240-6246 (2007).
14. Avramescu A, Andreescu S, Noguer T, Bala C, Andreescu D, Marty JL. Biosensors designed for environmental and food quality control based on screen-printed graphite electrodes with different configurations. Anal Bioanal Chem 374(1), 25-32 (2001).
15. Veira IC, Fatibello-Filho O. Biosensor based on paraffin/graphite modified with sweet potato tissue for the determination of hydroquinone in cosmetic cream in organic phase. Talanta 52(4), 681-689 (2000).
16. Hlavatá L, Vyskočil V, Beníková K, Borbélyová M, Labuda J. DNA-Based Biosensors with External Nafion and Chitosan Membranes for the Evaluation of the Antioxidant Activity of Beer, Coffee,

and Tea. Cent Eur J Chem 12, 604–611 (2014).
17. Hájková A, Barek J, Vyskočil V. Electrochemical DNA Biosensor for Detection of DNA Damage Induced by Hydroxyl Radicals. Bioelectrochemistry 116, 1–9 (2017).
18. Hlavatá L, Vyskočil V, Beníková K, Borbélyová M, Labuda J. DNA-Based Biosensors with External Nafion and Chitosan Membranes for the Evaluation of the Antioxidant Activity of Beer, Coffee, and Tea. Cent Eur J Chem 12, 604–611 (2014).
19. Hájková A, Barek J, Vyskočil V. Voltammetric Determination of 2-Aminofluoren-9-one and Investigation of Its Interaction with DNA on a Glassy Carbon Electrode. Electroanalysis 27, 101–110 (2015).
20. Raoof JB, Ojani R, Kiani A. Carbon paste electrode spiked with ferrocene carboxylic acid and its application to the electrocatalytic determination of ascorbic acid. J Electroanal Chem 515(1-2) 45 (2001).
21. Kato D, Sekioka N, Ueda A, Kurita R, Hirono S, Suzuki K, Niwa O. A Nanocarbon Film Electrode as a Platform for Exploring DNA Methylation. J Am Chem Soc 130(12), 3716-3717 (2008).
22. McCreery RL. Advanced Carbon Electrode Materials for Molecular Electrochemistry. Chem Rev 108(7), 2646-2687 (2008).
23. Daniel M, Francisco C, Esteve MF, Salvador A. Determination of organophosphorous and carbamate pesticides using a biosensor based on a polishable 7,7,8,8–tetracyanoquino-dimethane-modified, graphite- epoxy biocomposite. Anal Chim Acta 373(3), 305-313 (1997).
24. Bansal RC, Donnet JB, Stoeckli F. Active carbon, NewYork: Marcel Dekker, (1988).
25. Puri BR. In: Walker Jr. PJ, editor, Chemistry and physics of carbon, Vol. 6, New York: M. Dekker, p. 191 (1970).
26. Chowdhury ZZ, Zain SM, Khan RA, Khalid K. Process variables optimization for preparation and characterization of novel adsorbent from lignocellulocic waste. BioResources 7(3), 3732-375 (2012).
27. Mohan D, Sarswat A, Ok YS, Pittman CU. Organic and inorganic contaminants removal from water with biochar, renewable, low cost and sustainable adsorbent-A critical Review. Bioresour Technol 160, 192-202 (2014).
28. Wang Y, Yang RT. Desulfurization of Liquid Fuels by Adsorption on Carbon-Based Sorbents and Ultrasound-Assisted Sorbent Regeneration. Langmuir 23, 3825–3831 (2007).
29. Kovtyukhova NI, Ollivier PJ, Martin BR, Mallouk TE, Chizhik SA, Buzaneva EV, Gorchinskiy AD. Layer-by-Layer Assembly of Ultrathin Composite Films from Micron-Sized Graphite Oxide Sheets and Polycations. Chem Mater 11(3), 771-778 (1999).
30. Dékány I, Krüger-Grasser R, Weiss A. Selective liquid sorption properties of hydrophobized graphite oxide nanostructures. Colloid Polym Sci 276(7), 570-576 (1998).
31. Liu P, Gong K, Xiao P. Preparation and Characterization of Poly(vinyl acetate)-Intercalated Graphite Oxide. Carbon 37(12), 2073-2075 (1999).
32. Cassagneau T, Fendler HJ. High Density Rechargeable Lithium-Ion Batteries Self-Assembled from Graphite Oxide Nanoplatelets and Polyelectrolytes. J H Adv Mater10 877- 881 (1998).
33. Wu J, Zou Y, Li X, Liu H, Shen Guoli,Yu R. A biosensor monitoring DNA hybridization based on polyaniline intercalated graphite oxide nanocomposite. Sensors and Actuators B 104, 43–49 (2005).
34. Hummers WS, Offeman RE. Preparation of graphitic oxide. J Am Chem Soc 80, 1339-1345 (1958).
35. Bashkova S, Deoki D, Bandosz TJ. Effect of silver nanoparticles deposited on micro/mesoporous activated carbons on retention of NOx at room temperature. J Colloid Interface Sci 354, 331-340 (2011).
36. Triantafyllidis KS, Deliyanni EA. Desulfurization of diesel fuels: Adsorption of 4,6-DMDBT on different origin and surface chemistry nanoporous activated carbons. Chem Engin J 236, 406–414 (2014).
37. Boehm HP. Chemical identification of surface groups. Adv Catal 16, 179–274 (1966).
38. Palaska P, Aritzoglou E, Girousi S. Sensitive detection of cyclophosphamide using DNA-modified carbon paste, pencil graphite and hanging mercury drop electrodes Talanta 72, 1199-1206 (2007).
39. Girousi S, Serpi C, Karastogianni S. Voltammetry: A Promising Analytical Technique in the Study of Compounds of Biological Importance In Voltammetry: Theory, Types and Applications Authors/ Editors: Yuki Saito and Takumi Kikuchi, Nova Science Publishers, Inc (2013).
40. Kyzas GZ, Travlou NA, Deliyanni EA. The role of chitosan as nanofiller of graphite oxide for the removal oftoxic mercury ions. Colloids and Surf B: Biointerfaces 113, 467– 476 (2014).
41. Kyzas GZ, Lazaridis NK, Deliyanni EA. Oxidation time effect of activated carbons for drug adsorption. Cheml Eng J 234, 491-499 (2013).
42. Sharma S, Sanpui P, Chattopadhyay A, Ghosh SS. Fabrication of antibacterial silver nanoparticle-sodium alginate-chitosan composite films. RSC Advanc-

es 2, 5837–5843 (2012).
43. An J, Luo Q, Yuan X, Wang D, Li X. Preparation and characterization of silver-chitosan nanocomposite particles with antimicrobial activity. J Appl Polym Sci 120, 3180–3189 (2011).
44. Seung HH. Thermal reduction of graphene oxide, in: S. Mikhailov (Ed.), Physics and Applications of Graphene – Experiments, InTech, Rijeka, Croatia, pp.73–90 (2011).
45. Fuente E, Menéndez JA, Diez MA, Suárez D, Montes-Morán MA. Infrared Spectroscopy of Carbon Materials: A Quantum Chemical Study of Model Compounds. J Phys Chem B 107, 6350-6359 (2003).
46. Seredych M, Hulicova-Jurcakova D, Lu GQ, Bandosz TJ. Surface functional groups of carbons and the effects of their chemical character, density and accessibility to ions on electrochemical performance. Carbon 46, 1475- (2008).
47. Silverstein RM, Webster FX. Spectroscopic identification of organic compounds, John Wiley and Sons, New York, (1998).
48. Huang WX, White JM. Revisiting NO2 on Ag(111): a detailed TPD and RAIRS study. Surf Sci 529, 455-470 (2003).

Citation:
Karastogianni S, Deliyanni EA, Girousi S. Application of promising carbonaceous materials in electrochemical DNA sensing. J Appl Bioanal 3(4), 110-119 (2017).

Funding/Manuscript writing assistance:
The authors have no financial support or funding to report and they also declare that no writing assistance was utilized in the production of this article.

Competing interest:
The authors have declared that no competing interest exist.